


Chapter 5

Graphitization of Carbon Nanotubes Fabricated from Na@AAO Template Method

Abstract

In this work, we present a systematic study of the effects of graphitization on the structural perfection of CNT. High purity tubes were produced by a Na@AAO template method and subsequently annealed at 3073 K. The tubes were characterized for chemical purity, interlayer spacing, defect healing and structure. The structure transformation mechanism of CNT into graphite fibers is discussed to clarify the roles of the wall construction.

5.1 Introduction



After the discovery of CNT by Iijima in 1991,¹ their exceptional physical properties have generated a great deal of interests for possible applications in numerous fields.² Previously, the effect of high temperature annealing, or graphitization, of CNT has been extensively studied.³⁻⁶ It has been shown that the wall structure amenable to the formation of graphene layers undergoes structural reordering at high temperatures. But there were few reports describing the overall morphology change of CNT and other related carbon materials after graphitization. In this study, we wish to report interesting morphology changes of CNT fabricated from reactive template methods, employing Na filled anodic aluminum oxide (Na@AAO) to react with C₆Cl₆ and C₆F₆, after graphitization at 3073 K.

5.2 Experimental Section

Two types of CNT were fabricated by reacting Na@AAO with C₆Cl₆ and C₆F₆ inside a

tube furnace at 623 K.⁷⁻⁸ After immersed in 48 % HF at room temperature, the AAO template was removed. The CNT were subsequently heated inside a graphitization furnace at 1273 K for 1 h. Then, the furnace was put under automatic control and heated at a ramp rate 283 K/min to 3073 K and hold for 30 min under Ar flow. The samples were investigated by scanning electron microscope (SEM, JEOL JSM-6330F at 15 kV and HITACHI S-4000 at 25 kV) to observe morphological changes. The structure and texture changes of the samples were studied by a high-resolution transmission electron microscope (HRTEM, Philips TECNAI 20 at 200 kV). The crystallinity change after graphitization was investigated by an X-ray diffractometer (XRD, BRUKER AXS D8 ADVANCE) and a Raman spectrometer (Jabin-Yvon Raman Spectrometer T-64000).

5.3 Results and Discussion

Figure 5.1 shows electron micrographs of vertically aligned CNT grown from C_6Cl_6 and C_6F_6 via the Na@AAO membrane route at 623 K. Figures 5.1 (a) and 5.1 (b) show that the CNT grown from C_6Cl_6 are long, with smooth walls and a relatively homogeneous diameter of 335 nm. The electron diffraction (ED) pattern in Figure 5.1 (b) suggests that the material is amorphous. In contrast, the CNT fabricated from C_6F_6 has a porous wall and a uniform diameter of 320 nm. The material has a more crystallized graphite structure, as shown by the ED pattern in Figure 5.1 (d). Both of these results have been reported previously.⁷⁻⁸

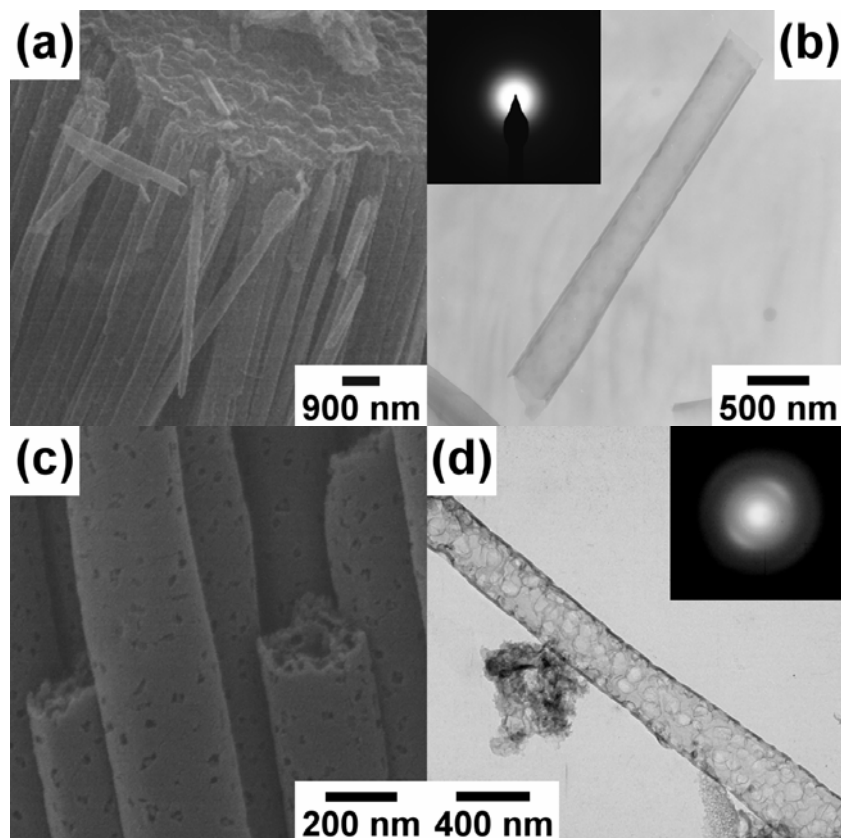


Figure 5.1 Images of a CNT array grown from C_6Cl_6 (a) SEM, (b) TEM and ED (inset); and from C_6F_6 (c) SEM, (d) TEM and ED (inset) after AAO is removed.

After graphitization at 3073 K, two morphologies were obtained for the sample prepared from C_6Cl_6 . One keeps the tubular structure with a diameter of 350 nm, as shown in Figure 5.2 (a). The other is carbon fibers (CF) shown in Figure 5.2 (b). Apparently, the CF is transformed from the CNT. The relative ratio between the CNT and the CF is estimated to be 1:9. The wall of the CNT becomes rough with defects on the surface. The CF shows diameters ranging from 70 – 175 nm and lengths of several μm . The TEM image in Figure 5.2 (c) also shows that the original smooth CNT wall structure becomes very rough. Figure 5.2 (d) shows TEM and HRTEM micrographs of a CF formed after the graphitization process. The TEM image shows a straight structure characteristic of a well-graphitized CF. A narrow channel of 5 nm is also discovered near the center axis of the fiber. The HRTEM image was taken from one side of the CF wall indicated by an arrow. The image demonstrates typical graphite layer

stacking with an average interlayer distance of 0.35 nm. The ED pattern illustrates a well-ordered graphite structure. From the pattern, an interlayer spacing of 0.35 nm is estimated. This is comparable to the spacing obtained from the HRTEM image. It also shows that the graphene layers parallel the long axis of the CF. In summary, the discussion above suggests that the high temperature process caused a large amount of the original α -CNT to collapse and to transform them into highly graphitized CF.

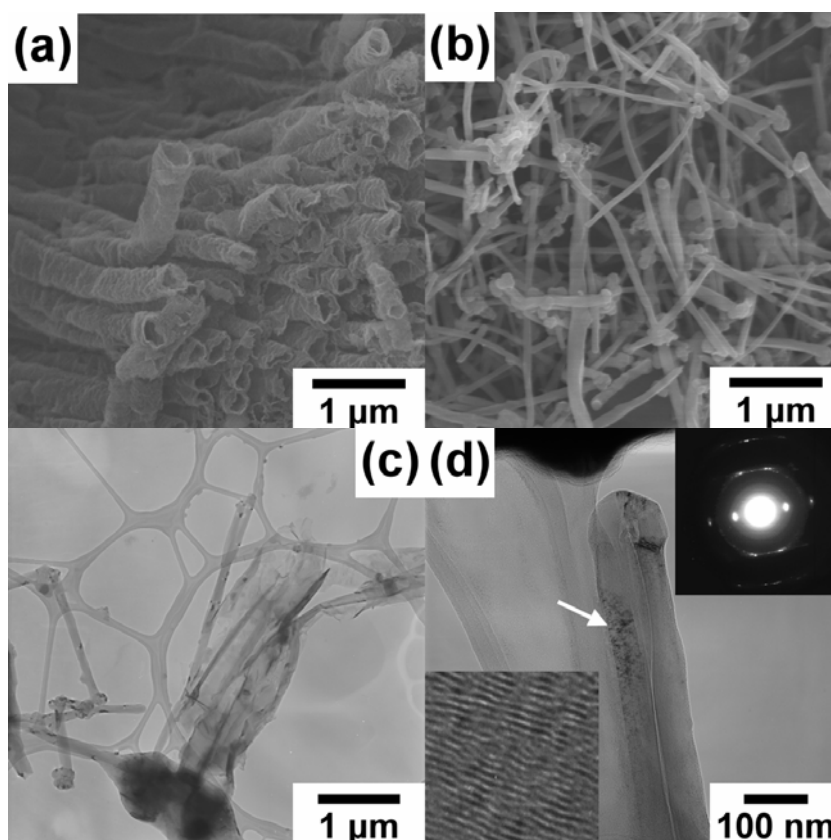


Figure 5.2 Morphology of the materials grown from C_6Cl_6 after annealed at 3073 K. SEM images of (a) CNT and (b) CF; (c) TEM image of a section of a CNT; and (d) TEM, HRTEM and ED (insets) of a CF.

For the porous CNT synthesized from C_6F_6 , both CNT and CFs were also found after graphitization, as shown in Figures. 5.3 (a) and 5.3 (b), respectively. Contrast to the CNT prepared from C_6Cl_6 , nearly half of the porous CNT maintained the original tubular structure and rough surface after graphitization. Only half of them were transformed into CFs. In

Figure 5.3 (c), TEM studies of the graphitized CNT are shown. The low magnification image shows that the CN has a porous tubular structure, which resembles the original CNT before the high temperature process. The only difference is that the walls are well-graphitized, as demonstrated by the ED and the HRTEM images in the insets in Figure 5.3 (c). From the ED pattern, an interlayer spacing of 0.36 nm is estimated. This is comparable to the spacing shown in the HRTEM image, 0.35 nm. In Figure 5.3 (d), the TEM studies of an isolated CF are shown. The fiber is straight with an average diameter of 125 nm. From the ED pattern (inset of Figure 5.3 (d)), an interlayer spacing of 0.35 nm is estimated. This concludes that the CF has a graphite structure with the graphene layers parallel the long axis of the CF. To sum up the above observations, it is apparent that the porous CNT prepared from C_6F_6 endured the high temperature process and withheld the original porous structure much better than the CNT synthesized from C_6Cl_6 .



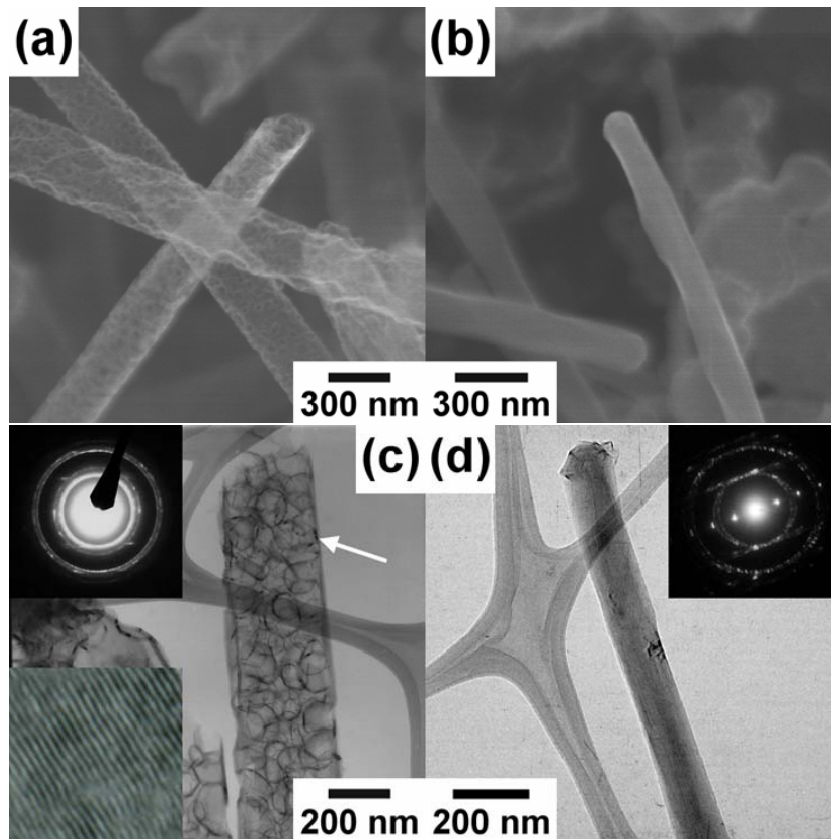


Figure 5.3 Morphology of the materials grown from C_6F_6 after annealed at 3073 K. SEM images of (a) CNT and (b) CFs; (c) TEM, HRTEM and ED (insets) of a section of a CNT; and (d) TEM and ED (inset) of a CF.

Figure 5.4 shows the XRD patterns of the graphitized CNT. The most obvious signals are the peaks corresponding to the reflections of highly ordered graphite (002) planes. This agrees with the TEM and the ED studies discussed above.

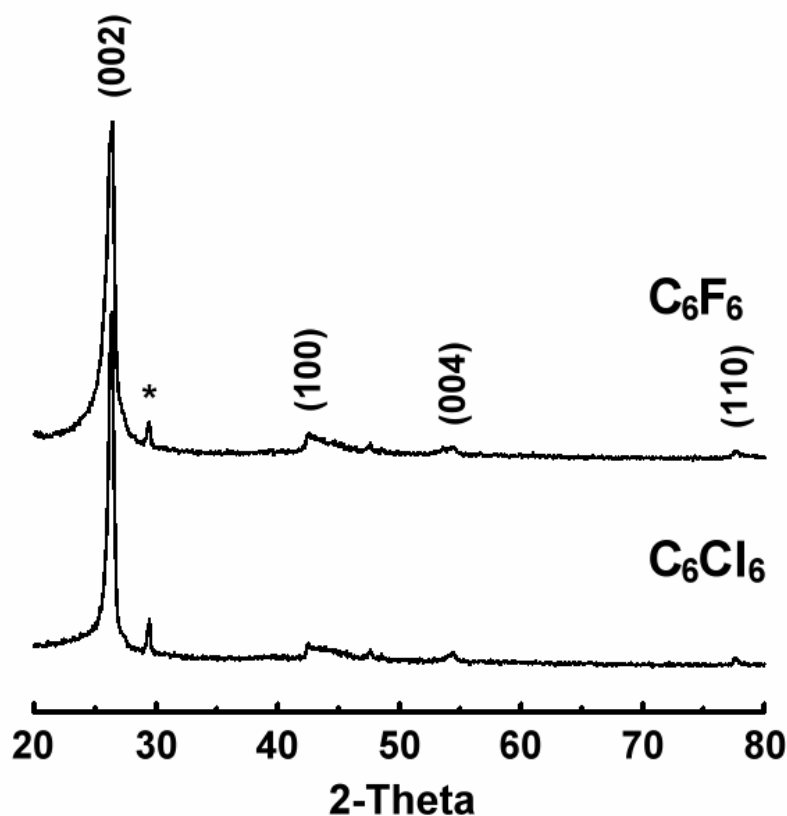


Figure 5.4 XRD of samples prepared from C_6Cl_6 and C_6F_6 after graphitization at 3073 K.

In Figure 5.5, Raman spectra of the samples before and after the high temperature processes are shown. In Figure 5.5 (a), for the *a*-CNT prepared from C_6Cl_6 at 623 K, two broad peaks centered at 1348 and 1584 cm^{-1} are assigned to the D-band and the G-band, respectively. The shapes of the peaks suggest that the structure is much less ordered than the graphite structure. After heating the CNT at 3073 K for 30 min, a weak D-band and a strong G-band are observed at 1343 and 1567 cm^{-1} , respectively. The I_D/I_G value is estimated to be 0.09, suggesting that a marked development of the graphite structure. A similar observation is shown in Figure 5.5 (b) for the samples grown from C_6F_6 . The I_D/I_G after heat-treatment at 3073 K is 0.16, larger than the value obtained from Figure 5.5 (a). This is consistent with the data discussed above. Apparently after the graphitization, the CF has a more ordered structure than the CNT does. For the sample processed from the *a*-CNT, grown from C_6Cl_6 , the CF to CNT ratio is much higher than that for the sample processed from the porous CNT

synthesized from C_6F_6 . Consequently, the data show undoubtedly a higher crystallinity for the product from C_6Cl_6 than for the product from C_6F_6 .⁹

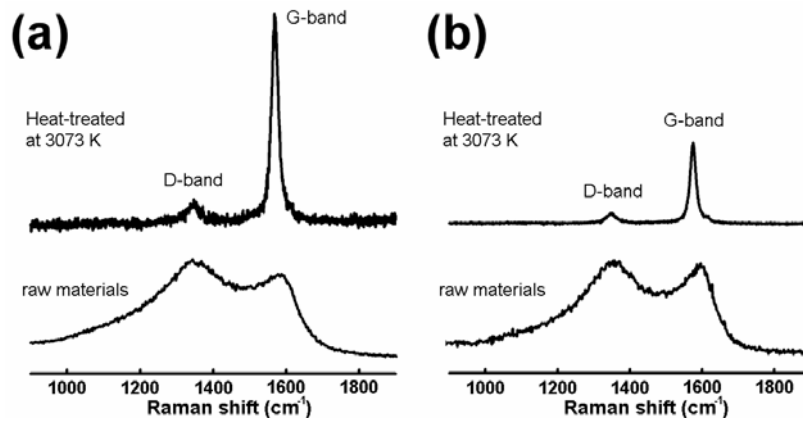


Figure 5.5 Raman spectra of samples grown from (a) C_6Cl_6 and (b) C_6F_6 before and after heat treatment at 3073 K.

5.4 Conclusion

In summary, graphitization of the *a*-CNT and the porous CNT generated both tubular and fibrous products but with different yields. A possible explanation for the phenomenon is rooted in the original structure of the tubes.¹⁰⁻¹¹ Apparently, the CNT with a porous structure is structurally stronger and more resistant to the collapsing of the tube walls than the CNT with a hollow tubular structure. The later does not have the internal support and probably collapse more easily to form CF at high temperature. The study shows the importance of the micromorphology to the structural transformation in a high temperature process.

References

1. Iijima, S. *Nature* **1991**, 354, 56.
2. Baughman, R. H.; Zakhidov, A. A.; de Heer, W. A. *Science* **2002**, 297, 787.
3. Hamwi, A.; Alvergnat, H.; Bonnamy, S.; Beguin, F. *Carbon* **1997**, 35, 723.
4. Endo, M.; Saito, R.; Dresselhaus, M. S.; Dresselhaus, G. In: Ebbesen TW, editor, *Carbon nanotubes: preparation and properties*, Boca Raton, FL: CRC Press, 1997, pp.35–110.
5. Kyotani, T.; Tsai, L.; Tomita, A. *Chem. Mater.* **1996**, 8, 2109.
6. Andrews, R.; Jacques, D.; Qian, D.; Dickey, E. C. *Carbon* **2001**, 39, 1681.
7. Wang, L.-S.; Lee, C.-Y.; Chiu, H.-T. *Chem. Comm.* **2003**, 1964.
8. Huang, C.-H.; Chang, Y.-H.; Wang, H.-W.; Cheng, S.; Lee, C.-Y.; Chiu, H.-T. Carbon submitted.
9. Katagiri, G.; Ishida, H.; Ishitani, A. *Carbon* **1988**, 26, 565.
10. Noda, T.; Kato, H. *Carbon* **1965**, 3, 289.
11. Okabe, K.; Shiraishi, S.; Oya, A. *Carbon* **2004**, 42, 667.